 MCB, vol.10, no.3, pp.233-244, 2013

Numerical Modeling of Skin Tissue Heating Using the Interval Finite Difference Method

B. Mochnacki*, **Alicja Piasecka Belkhayat**†

Abstract: Numerical analysis of heat transfer processes proceeding in a non-homogeneous biological tissue domain is presented. In particular, the skin tissue domain subjected to an external heat source is considered. The problem is treated as an axially-symmetrical one (it results from the mathematical form of the function describing the external heat source). Thermophysical parameters of sub-domains (volumetric specific heat, thermal conductivity, perfusion coefficient etc.) are given as interval numbers. The problem discussed is solved using the interval finite difference method basing on the rules of directed interval arithmetic, this means that at the stage of FDM algorithm construction the mathematical manipulations are realized using the interval numbers. In the final part of the paper the results of numerical computations are shown, in particular the problem of admissible thermal dose is analyzed.

1 Introduction

The domain of skin tissue can be treated as a heterogeneous one being the composition of layers corresponding to the epidermis, dermis and sub-cutaneous region – Figure 1 [1]. The thicknesses of layers and also the thermophysical parameters of sub-domains are individual personal traits and this fact suggests the application of interval arithmetic methods at the stage of numerical modeling of the process analyzed.

So, the considerations presented below concern imprecisely defined transient bio-heat transfer problems, when in the mathematical description the uncertain parameters are defined and treated as directed interval numbers (e.g. [2, 3, 4]). The base of mathematical model is given by the Pennes interval set of equations supplemented by the adequate boundary-initial conditions.

* Higher School of Labour Safety Management at Katowice, Poland.
Email: bohdan.mochnacki@im.pcz.pl
† Silesian University of Technology, Gliwice, Poland.
Email: alicja.piasecka@polsl.pl

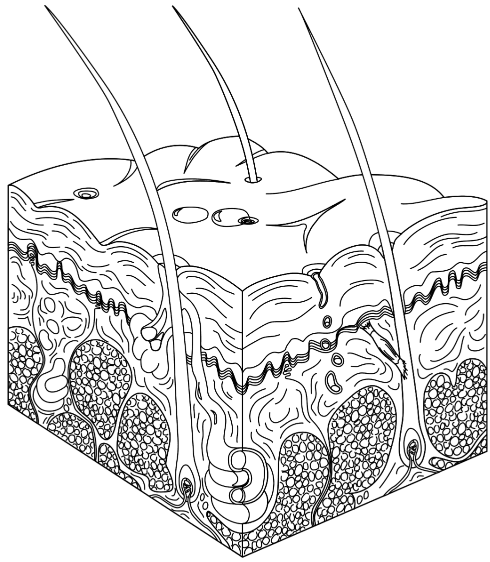

Figure 1: Skin tissue

The numerical solution of the problem discussed gives, among others, the information concerning the possibility of thermal destruction of the tissue. This process can take place when the temperature corresponding to the surface between epidermis and dermis exceeds the value of 44°C. The thermal damage of the biological tissue (burn degree) can be found using the first order Arrhenius equation (Henriques burn integral [5, 6]).

The thermal energy supplied to the surface of the skin tissue (the thermal dose) can be found using the formula

$$TD = \int_0^{t_p} \int_\Omega q_B \, \mathrm{d}\Omega \, \mathrm{d}t \tag{1}$$

where q_B is the function describing the boundary heat flux, Ω is the surface of heat flux action, t_p is the exposure time. For $t > t_p$ on the surface considered the Robin condition should be taken into account. In this paper the results obtained using the interval FDM have been used to determine the admissible thermal dose at which the tissue remains in a natural state.

2 Governing equations

Thermal processes proceeding in the heterogeneous skin tissue domain can be described by the following system of interval energy equations [1, 7]

$$\left[c_e^-,\, c_e^+\right] \frac{\partial T_e(r,z,\ t)}{\partial t} = \left[\lambda_e^-,\, \lambda_e^+\right] \nabla^2 T_e(r,z,\ t) + \left[Q_e^-(r,z,t),\, Q_e^+(r,z,\ t)\right] \tag{2}$$

where e = 1, 2, 3 corresponds to the successive layers of skin (epidermis, dermis, subcutaneous region), $[\lambda_e^-,\ \lambda_e^+]$ is the interval thermal conductivity, signs '–' and '+' correspond to the lower and upper limits of interval number, $[c_e^-,\ c_e^+]$ is the interval volumetric specific heat, $[Q_e^-(x,t),\ Q_e^+(x,t)]$ is the capacity of interval internal heat sources, $T_e(r,z,\ t)$, r,z and t denote the temperature, spatial co-ordinates and time.

The capacity of interval internal heat sources is a sum of two components

$$[Q_e^-(r,z,t),\ Q_e^+] = [G_{Be}^-,\ G_{Be}^+]\, c_{Be}\, [T_B - T_e(r,z,t)] + [Q_{me}^-,\ Q_{me}^+] \tag{3}$$

where $[G_{Be}^-,\ G_{Be}^+]$ is the interval perfusion coefficient, c_B is the volumetric specific heat of blood, T_B is the arterial blood temperature, $[Q_{me}^-,\ Q_{me}^+]$ is the interval metabolic heat source.

Interval equations (2) should be supplemented by the boundary and initial conditions. So, the skin surface ($r \le R,\ t < t_p$) is subjected to an external heat source, for $t > t_p$ the boundary condition of the 3^{rd} type (the continuity of boundary heat flux) is assumed, while for the others parts of the boundary the no-flux conditions are taken into account

$$\begin{cases} x \in \Gamma_0,\ r \le R, \quad t \le t_p: & \bar{q}(r,z,\ t) = -\left[\lambda_1^-,\ \lambda_1^+\right] \frac{\partial T_1(r,z,t)}{\partial n} = \bar{q}_B \\ x \in \Gamma_0,\ r \le R, \quad t > t_p: & -\left[\lambda_1^-,\ \lambda_1^+\right] \frac{\partial T_1}{\partial n} = \alpha \left[T_1^{(}r,z,t) - T_a\right] \\ x \in \Gamma_\infty: & -[\lambda_e^-,\ \lambda_e^+] \frac{\partial T_e(r,z,t)}{\partial n} = \bar{0} \end{cases} \tag{4}$$

where $\bar{q}_B$ is the given interval boundary heat flux, α is the heat transfer coefficient, T_a is the ambient temperature, $\partial T_e / \partial n$ is the normal derivative.

Between the successive sub-domains the continuity condition is assumed

$$x \in \Gamma_e: \quad \begin{cases} -[\lambda_e^-, \lambda_e^+] \frac{\partial T_e(r,z,\ t)}{\partial n} = -[\lambda_{e+1}^-, \lambda_{e+1}^+] \frac{\partial T_{e+1}(r,z,\ t)}{\partial n} \\ T_e(r,z,\ t) = T_{e+1}(r,z,\ t) \end{cases} \tag{5}$$

The initial condition is also given

$$t = 0: \quad T_e(r,z,\ 0) = T_{0e}(r,z) \tag{6}$$

The equations (2) – (6) create the mathematical model of the process discussed.

The problem formulated has been solved by means of interval finite difference method using the rules of directed interval arithmetic [7, 8]. In this arithmetic the set of proper intervals is extended by the improper intervals: it is possible to obtain the number zero by subtraction of two identical intervals and the number one as the result of division [2, 4, 9]. The directed interval arithmetic seems to be more effective at the stage of numerical algorithm construction.

3 Numerical algorithm

The domain considered is shown in Figure 2.

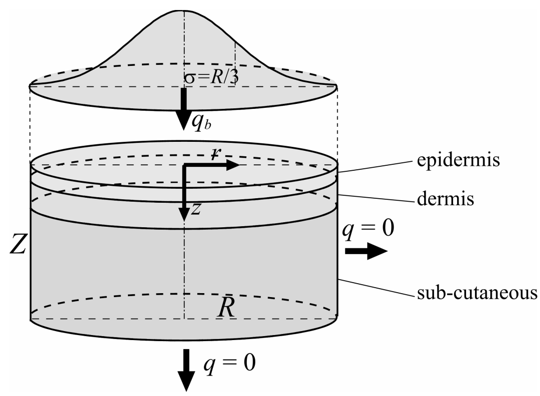

Figure 2: Domain considered

At first, the time grid is introduced

$$t^0 < t^1 < ... < t^{f-2} < t^{f-1} < t^f < ... < t^F < \infty \tag{7}$$

with a constant step Δt .

The domain is covered by the regular geometrical mesh and the 5-points stars created by the central node (i, j) and the adjoining ones are considered (Figure 3). The ‘boundary’ nodes are located at the distance $0.5h$ or $0.5k$ with respect to the real boundary (h,k are the steps of regular mesh in directions r and z), respectively. This approach gives the better approximation of the Neumann and Robin boundary conditions [10].

The final form of FDM equation (the explicit scheme) for the internal nodes is the

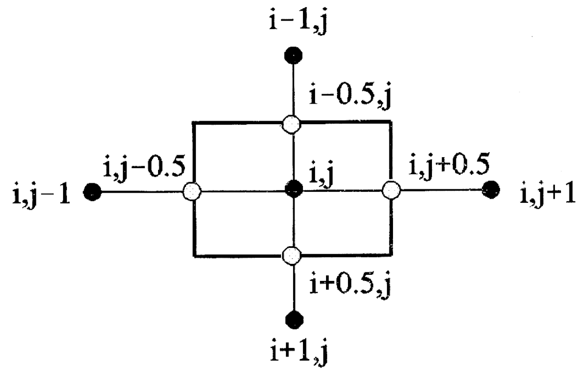

Figure 3: Five-points star

following (the approach close to the algorithm presented in [7, 11] is used)

$$
\begin{aligned}
&\bar{c}_{i,j}^{f-1}\frac{\bar{T}_{i,j}^{f}-\bar{T}_{i,j}^{f-1}}{\Delta t}=\frac{\Phi_{i,j-1}}{\bar{R}_{i,j-1}^{f-1}}\left(\bar{T}_{i,j-1}^{f-1}-\bar{T}_{i,j}^{f-1}\right)+\frac{\Phi_{i,j+1}}{\bar{R}_{i,j+1}^{f-1}}\left(\bar{T}_{i,j+1}^{f-1}-\bar{T}_{i,j}^{f-1}\right)+\\
&\frac{\Phi_{i-1,j}}{\bar{R}_{i-1,j}^{f-1}}\left(\bar{T}_{i-1,j}^{f-1}-\bar{T}_{i,j}^{f-1}\right)+\frac{\Phi_{i+1,j}}{\bar{R}_{i+1,j}^{f-1}}\left(\bar{T}_{i+1,j}^{f-1}-\bar{T}_{i,j}^{f-1}\right)+\left(\bar{Q}_{p}\right)_{i,j}^{f-1}+\left(\bar{Q}_{m}\right)_{i,j}^{f-1}
\end{aligned}
\tag{8}
$$

where

$$
\bar{R}_{i,j+1}^{f-1}=\frac{0.5h}{\bar{\lambda}_{i,j}^{f-1}}+\frac{0.5h}{\bar{\lambda}_{i,j+1}^{f-1}},\quad \bar{R}_{i,j-1}^{f-1}=\frac{0.5h}{\bar{\lambda}_{i,j}^{f-1}}+\frac{0.5h}{\bar{\lambda}_{i,j-1}^{f-1}}
\tag{9}
$$

and

$$
\bar{R}_{i+1,j}^{f-1}=\frac{0.5k}{\bar{\lambda}_{i,j}^{f-1}}+\frac{0.5k}{\bar{\lambda}_{i+1,j}^{f-1}},\quad \bar{R}_{i-1,j}^{f-1}=\frac{0.5k}{\bar{\lambda}_{i,j}^{f-1}}+\frac{0.5k}{\bar{\lambda}_{i-1,j}^{f-1}}
\tag{10}
$$

are the thermal resistances between central node and the adjoining ones (the rules concerning the mathematical operations defined for interval numbers must be taken into account, of course). For example, the thermal resistance $i, j+1$ should be calculated according to the formula (the example presented below is rather a simple one)

$$
\begin{aligned}
&\bar{R}_{i,j+1}^{f-1}=\frac{0.5h}{\bar{\lambda}_{i,j}^{f-1}}+\frac{0.5h}{\bar{\lambda}_{i,j+1}^{f-1}}=\frac{0.5h}{\left[\lambda_{i,j}^{-},\,\lambda_{i,j}^{+}\right]^{f-1}}+\frac{0.5h}{\left[\lambda_{i,j+1}^{-},\,\lambda_{i,j+1}^{+}\right]^{f-1}}=\\
&\left[\frac{0.5h}{\lambda_{i,j}^{-}},\,\frac{0.5h}{\lambda_{i,j}^{+}}\right]^{f-1}+\left[\frac{0.5h}{\lambda_{i,j+1}^{-}},\,\frac{0.5h}{\lambda_{i,j+1}^{+}}\right]^{f-1}=\left[\frac{0.5h}{\lambda_{i,j}^{-}}+\frac{0.5h}{\lambda_{i,j+1}^{-}},\,\frac{0.5h}{\lambda_{i,j}^{+}}+\frac{0.5h}{\lambda_{i,j+1}^{+}}\right]^{f-1}
\end{aligned}
$$

(11)

In turn

$$\Phi^{=}_{i,j-1}\tfrac{r_{i,j}-0.5h}{r_{i,j}h},\quad \Phi^{=}_{i,j+1}\tfrac{r_{i,j}+0.5h}{r_{i,j}h},\quad \Phi^{=}_{i-1,j}\Phi^{=}_{i+1,j}\tfrac{1}{k} \tag{12}$$

are the shape functions of differential mesh ($r_{i,j}$ is the radial co-ordinate of node (i,j)).

Using the equation (8) the temperature at the point (i,j) for time level f can be found under the assumption that the stability condition for explicit differential scheme is fulfilled [10]. It should be pointed out that the equation (8) takes effect both in the case of 'homogeneous' stars and also when the nodes creating the star belong to the different sub-domains (boundary condition (5)).

It can be shown that the only change of equation (8) for the nodes located close to the external boundary for which the boundary condition (4b) is given reduces to the redefinition of the adequate thermal resistance. If, for instance, the direction to the external boundary corresponds to $i, j+1$ then

$$\bar{R}^{f-1}_{i,j+1} = \frac{0.5h}{\bar{\lambda}^{f-1}_{i,j}} + \frac{1}{\alpha} \tag{13}$$

at the same time the ambient temperature plays a role of temperature $T^{f-1}_{i,j+1}$. The no-flux condition can be taken into account assuming very small value of heat transfer coefficient, e.g. $\alpha = 10^{-10}(\bar{R}^{f-1}_{i,j+1} \to \infty)$.

The FDM equation for the nodes close to the external boundary for which the Neumann condition (4a) is given takes a form ('to boundary' direction corresponds to i-1, j)

$$\begin{aligned}\bar{c}^{f-1}_{i,j}\frac{\bar{T}^{f}_{i,j}-\bar{T}^{f-1}_{i,j}}{\Delta t} &= \frac{\Phi_{i,j-1}}{\bar{R}^{f-1}_{i,j-1}}\left(\bar{T}^{f-1}_{i,j-1}-\bar{T}^{f-1}_{i,j}\right)+\frac{\Phi_{i,j+1}}{\bar{R}^{f-1}_{i,j+1}}\left(\bar{T}^{f-1}_{i,j+1}-\bar{T}^{f-1}_{i,j}\right)+\\ &(q_B)^{f-1}_{i,j}\Phi_{i-1,j}+\frac{\Phi_{i+1,j}}{\bar{R}^{f-1}_{i+1,j}}\left(\bar{T}^{f-1}_{i+1,j}-\bar{T}^{f-1}_{i,j}\right)+\left(\bar{Q}_p\right)^{f-1}_{i,j}+\left(\bar{Q}_m\right)^{f-1}_{i,j}\end{aligned} \tag{14}$$

As mentioned, the mathematical manipulations leading to the designation of temperature field corresponding to time level f should be done according to the rules of directed interval arithmetic.

4 Results of computations

The external heat flux is assumed in the form of the Gauss-type function

$$r \in [0,R], \quad t \le t_p: \quad q_b(r,0,t) = q_0 \exp\left[-\frac{r^2}{2(R/3)^2}\right] \tag{15}$$

where $R/3=\sigma$ is the standard deviation of a normal distribution of heat source, q_0 is the factor corresponding to the maximum incident heat flux, t_p is the exposure time.

The knowledge of function describing the boundary heat flux allows one to find the thermal dose, this means

$$TD = \int_0^{t_p}\int_0^{2\pi}\int_0^{R} q_0 \exp\left[-\frac{r^2}{2\,(R/3)^2}\right]\cdot r\,\mathrm{d}r\,\mathrm{d}\varphi\,\mathrm{d}t \tag{16}$$

in other words

$$TD = \frac{2\,\pi\,(1-\exp(-9/2))}{9} t_p\, q_0\, R^2 \approx 0.69\, t_p\, q_0\, R^2 \tag{17}$$

At the stage of numerical computations a three-layered cylindrical skin tissue domain of dimension Z = 12.1 mm and R = 20 mm has been considered. Additionally the following input data have been introduced: L_1 = 0.1 mm, L_2 = 2 mm, L_3 = 10 mm (where e = 1, 2, 3 correspond to the successive layers of skin – epidermis, dermis, sub-cutaneous region), λ_1= 0.235 W/(m·K), λ_2= 0.445 W/(m·K), λ_3= 0.185 W/(m·K), c_1= 4.3068·10^6 J/(m^3·K), c_2= 3.96·10^6 J/(m^3·K), c_3= 2.674·10^6 J/(m^3·K), c_B= 3.9962·10^6 J/(m^3·K), T_B= 37 ˚C, G_{B1}= 0, $G_{B2} = G_{B3}$= 0.00125 (m^{3}blood/s)/m^{3}tissue, $Q_{m1} = 0$, $Q_{m2} = Q_{m3}$= 245 W/m^3, initial temperature $T_{10} = T_{20} = T_{30}$= 37 ˚C, ambient temperature T_a= 37 ˚C, α =10 W/(m^{2}K). The mean parameters of skin tissue sub-domains are taken from [1].

Thermophysical parameters of successive layers are assumed as the interval ones, in particular

$$\bar{c}_e = [c_e - 0.05\,c_e,\; c_e + 0.05\,c_e]\,,\;\; \bar{\lambda}_e = [\lambda_e - 0.05\,\lambda_e,\; \lambda_e + 0.05\,\lambda_e]\,,\;\; e = 1,\,2,\,3.$$

Using the trial and error approach is calculated that the temperature at the point (L_1, 0) reached the critical value for the external heat flux 10 kW/m^2 and exposure time 1.042 s. For above parameters TD = 2.9 KJ. It should be pointed out that the critical temperature of skin tissue equals 44°C. This temperature can cause the burn of tissue. The interval solution obtained is shown in Figure 4.

For the same thermal doses but the other values of boundary heat fluxes and exposure times the differences between numerical solutions are visible. For example in Figures 5 and 6 the solutions for which the critical temperature is not reached are shown.

The next stage of investigations consisted in the designation of exposure time for the given boundary heat flux to obtain the critical temperature, at the same time

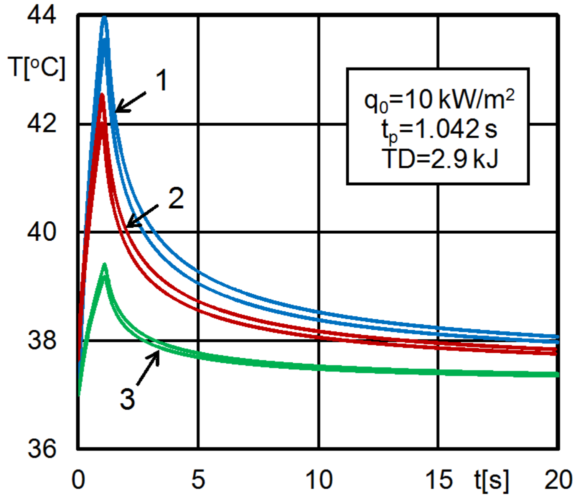

Figure 4: Heating/cooling curves at the points $1(L_1, 0)$, $2(L_1, R/4)$, and $3(L_1, R/2)$

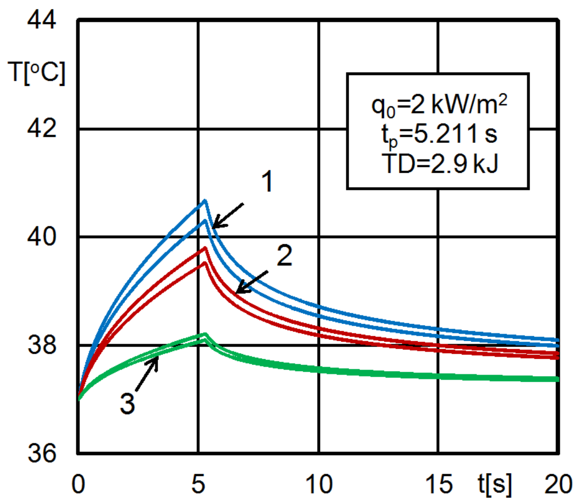

Figure 5: Heating/cooling curves at the points : $1(L_1, 0)$, $2(L_1, R/4)$, and $3(L_1, R/2)$ for the other boundary parameters and the same TD

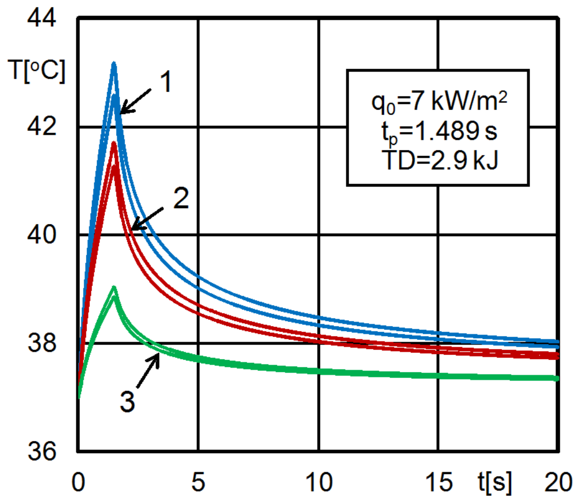

Figure 6: Heating/cooling curves at the points : $1(L_1,\, 0)$, $2(L_1,\, R/4)$, and $3(L_1,\, R/2)$ for the other boundary parameters and the same TD

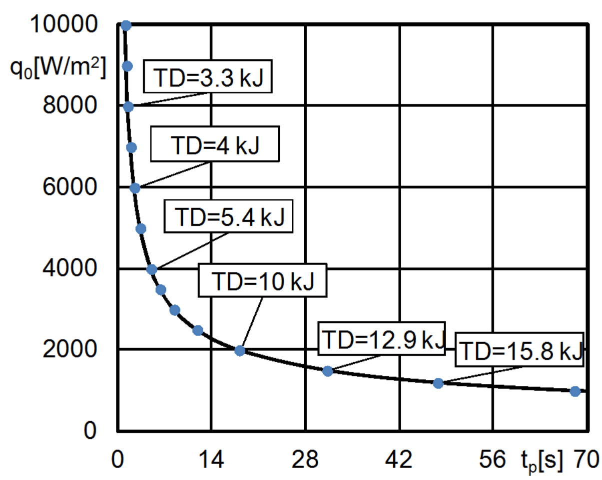

Figure 7: The admissible external heat flux parameters

the node 1 has been taken into account and $\bar{c}_e = [c_e - 0.05\, c_e,\, c_e + 0.05\, c_e]$, $\bar{\lambda}_e = [\lambda_e - 0.05\, \lambda_e,\, \lambda_e + 0.05\, \lambda_e]$, $e = 1,\, 2,\, 3$.

The results of numerical simulations are shown in Figure 7, while the selected solutions – in Figures 8 and 9.

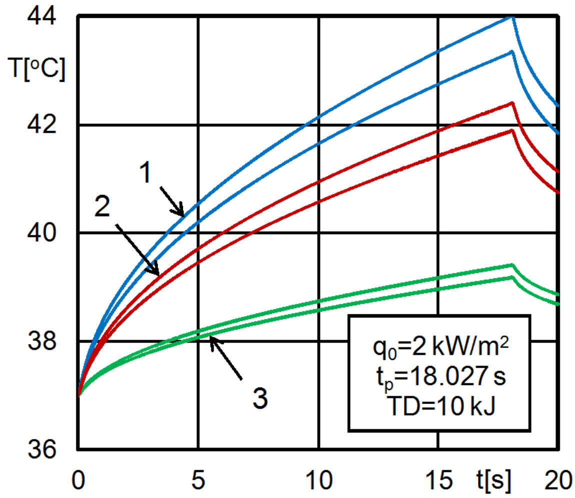

Figure 8: Heating/cooling curves at the points : $1(L_1, 0)$, $2(L_1, R/4)$, and $3(L_1, R/2)$ for the selected boundary parameters and TD=10KJ

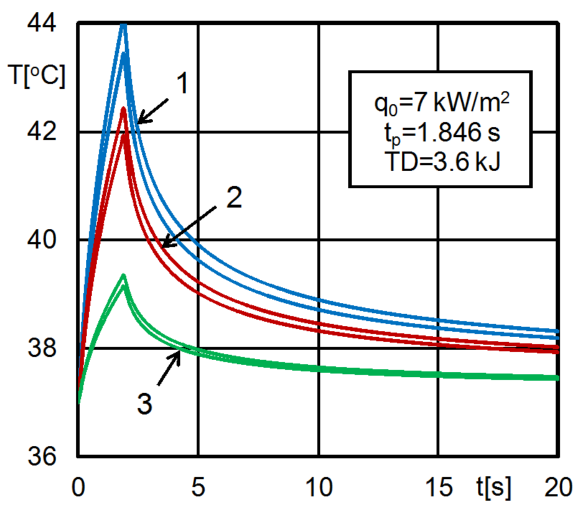

Figure 9: Heating/cooling curves at the points : $1(L_1, 0)$, $2(L_1, R/4)$, and $3(L_1, R/2)$ for the selected boundary parameters and TD=3.6KJ

5 Final remarks

The main aim of the research described in this paper was to present the possibilities of interval arithmetic application at the stage of FDM algorithm construction. In particular the non-steady bio-heat transfer proceeding in the non-homogeneous domain of skin tissue has been discussed. The generalization of FDM allows one to find the numerical solution in an interval form and such an information may be important, among other, in the medical practice. The results obtained have been compared with the classical FDM solution and this solution is located in the designed intervals [7].

To verify the effectiveness and exactness of solutions obtained the problem of the so-called admissible thermal dose has been selected. The testing computations show that the same thermal dose does not assure similar thermal effects. The process of tissue heating is determined first of all by the values of boundary heat flux and exposure time, while resulting from these parameters values of thermal doses are not an effective tool for the prediction of admissible tissue temperature appearance. This problem requires the further studies, of course, but it seems that from the physical point of view a such information is a significant one. The next stage of research will be connected with the modeling of tissue heating including the insulating properties of protective clothing [12] and also the application of the bio-heat transfer model basing on the dual phase lag approach [13].

Acknowledgements

This paper is part of project NR-13-0124-10/2010 and grant PB3/2013 realized at the WSZOP.

References

1. Majchrzak, E., (2012) *Biomechanics*, Vol. XII, Polish Academy of Sciences. Warsaw.

2. Markov, S.-M. (1995) On directed interval arithmetic and its applications, *Journal of Universal Computer Science*, 1, 514-526.

3. Piasecka, Belkhayat, A. (2011) Interval boundary element method for 2D transient diffusion problem using directed interval arithmetic, *Engineering Analysis with Boundary Elements*, 35, 3, Elsevier, 259-263.

4. Popova, E.-D. (2011) Multiplication Distributivity of Proper and Improper Intervals, *Reliable Computing*, 7, 129-140.

5. Majchrzak, E., Jasinski, M. (2004) Sensivity analysis of burns integrals, *Computer Assisted Mechanics and Engineering Sciences*, 11, 2/3, 125-136.

6. Majchrzak, E., Mochnacki, B. (2001) Analysis of bio-heat transfer in the system of blood vessel-biological tissue, *Kluver Academic Publishers*, 201-211.

7. Mochnacki, B., Piasecka, Belkhayat, A. (2012) Application of interval FDM in numerical modeling of bio-heat transfer, *International Conference*, *ECCOMAS Special Interest Conference, Wroclaw, Poland*, 4-6 September, CD-ROM Proceedings,1-10.

8. Jankowska, M.-A., Sypniewska-Kaminska, G. (2012) Interval Finite Difference Method for Bioheat Transfer Problem Given by the Pennes Equation with Uncertain Parameters, *Mechanics and Control*, 31, 2, 77-84.

9. Dawood, H. (2011) Theories *of Interval Arithmetic: Mathematical Foundations and Applications*, LAP LAMBERT Academic Publishing GmbH & Co., Germany.

10. Mochnacki, B., Suchy, J.-S. (1995) *Numerical methods in computations of foundry processes*, PFTA, Cracow.

11. Majchrzak, E., Mochnacki, B. (2004) *Numerical methods. Theoretical Base, practical aspects, algorithms*. Publ. of the Silesian Univ. of Technology, Gliwice.

12. Chitrphiromsn, P., Kuznetsov, A.-V. (2005) Modeling heat and moisture transport in firefighter protective clothing during flash fire exposure, Heat and Mass Transfer, 41, 206-215.

13. Liu, K.-C, Wang, Y.-N., Chen, Y.-S. (2012) Investigation of the bio-heat transfer with the dual-phase-lag effect, *International Journal of Thermal Science*, 58, 29-35.